Gas Phase Reactions

Heating: furnace, laser, plasma, flame, arc

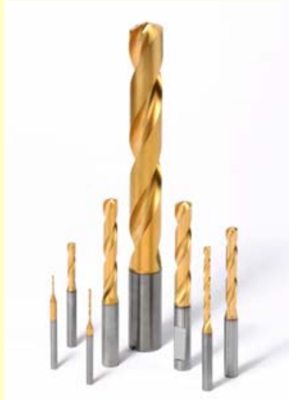

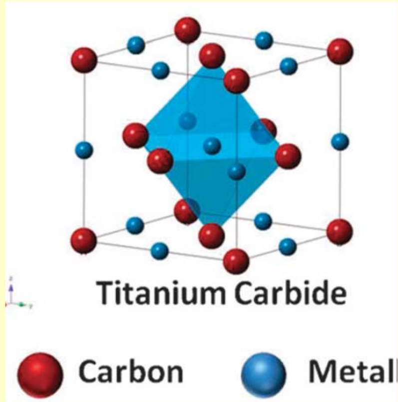

Gas-Metal Rxn

$Ti + N_2 \rightarrow TiN$ 1800 K

$Ti + CH_4 \rightarrow TiC + H_2$ mp 2940 °C

$3\,Si + 2\,N_2 \rightarrow Si_3N_4$

$W + CH_4 \rightarrow WC + H_2$ mp 2720 °C

WC dissolved in Co = cemented carbides (Widia materials)

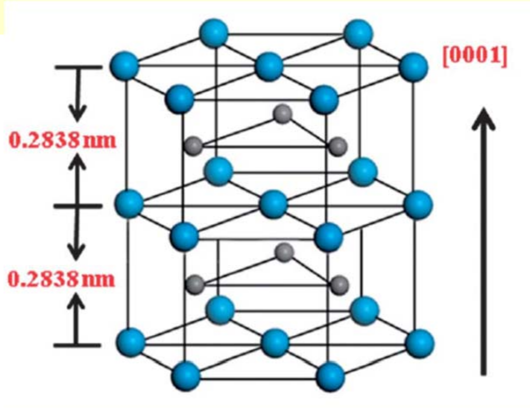

Cementite

$steel + H_2/CO + CH_4 + NH_3 \rightarrow Fe_3C + nitrides$

Gas Phase Reactions

Gas-Gas Rxn

Flame hydrolysis

volatile compounds are passed through an oxygen-hydrogen stationary flame, homogeneous nucleation from supersaturated vapor (nano):

$$SiCl_4 + 2\,H_2 + O_2 \rightarrow SiO_2 + 4\,HCl$$

fumed silica

Reagent	bp/°C	Product
$SiCl_4$	57	SiO_2
$AlCl_3$	180 (subl.)	Al_2O_3
$TiCl_4$	137	TiO_2
CrO_2Cl_2	117	Cr_2O_3
$Fe(CO)_5$	103	Fe_2O_3
$GeCl_4$	84	GeO_2
$Ni(CO)_4$	42	NiO
$SnCl_4$	114	SnO_2
$ZrCl_4$	331 (subl.)	ZrO_2
$VOCl_3$	127	V_2O_5

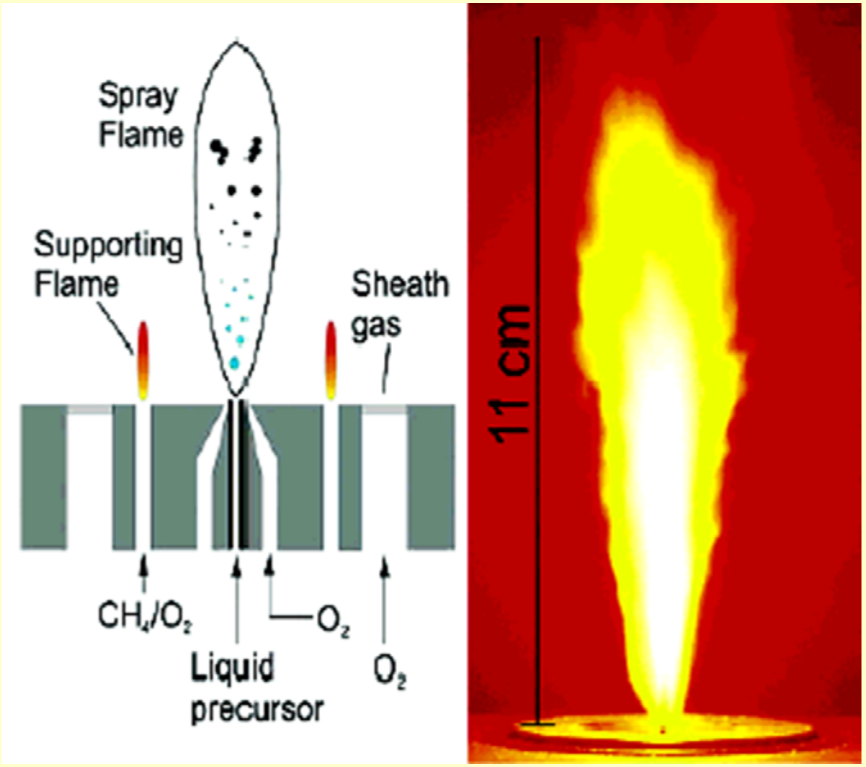

Gas Phase Reactions

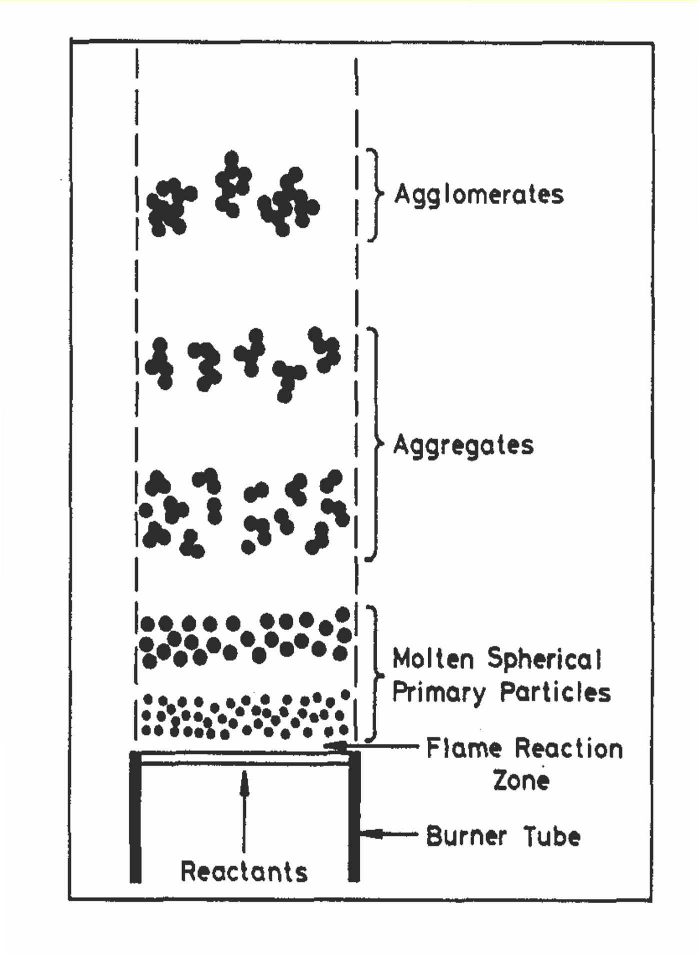

$SiCl_4 + H_2O \rightarrow OSiCl_2 + 2\,HCl$

$OSiCl_2 + H_2O \rightarrow SiClOOH + HCl$

$SiClOOH \longrightarrow \longrightarrow \longrightarrow \longrightarrow SiO_2 + HCl$

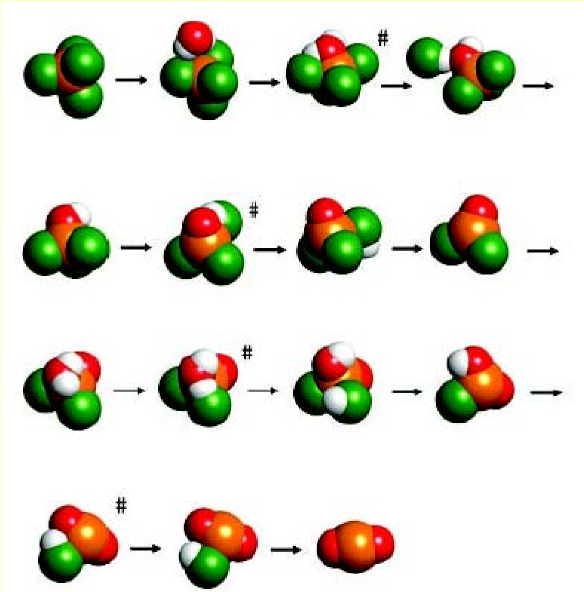

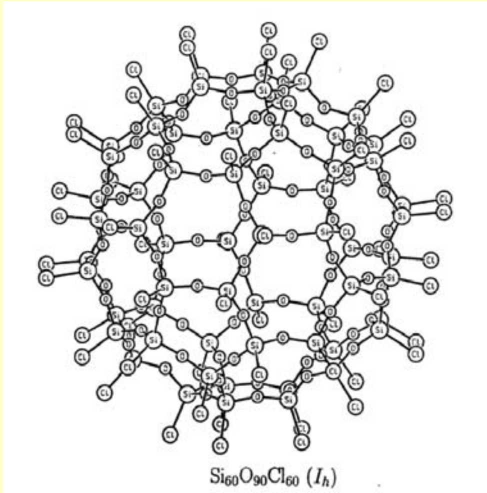

$Si_{60}O_{90}Cl_{60}$

Y_2O_3 Particles by Flame Aerosol Process

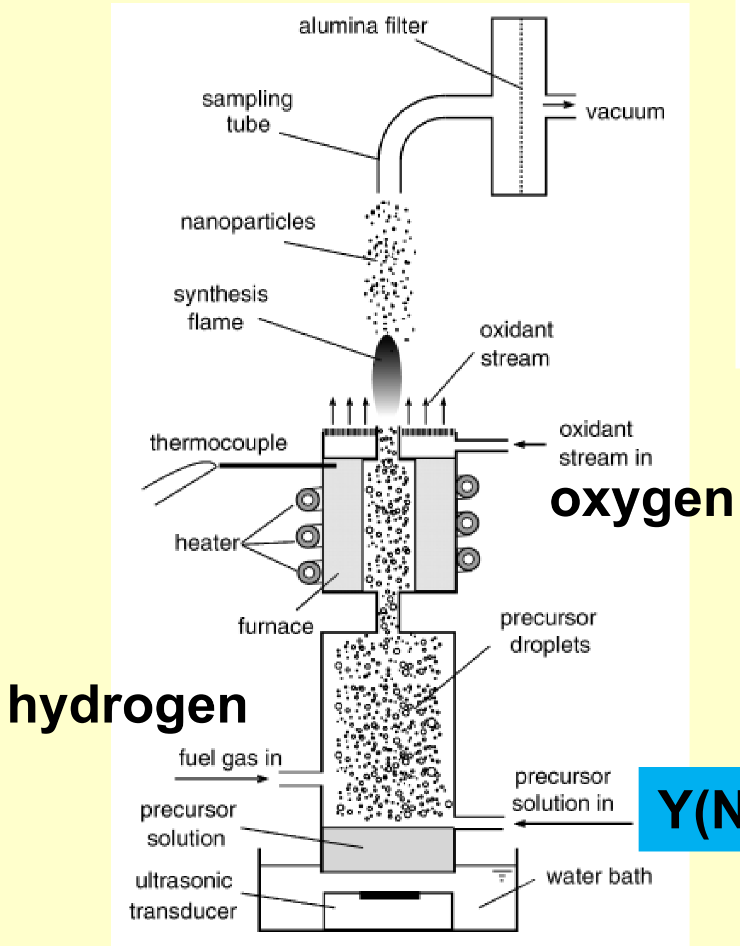

$Y(NO_3)_3$

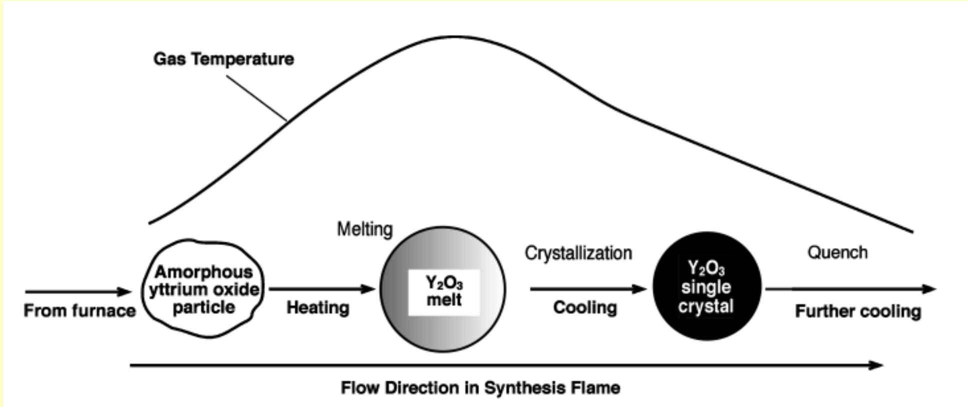

Particle size control by precursor concentration
Higher concentration = larger size

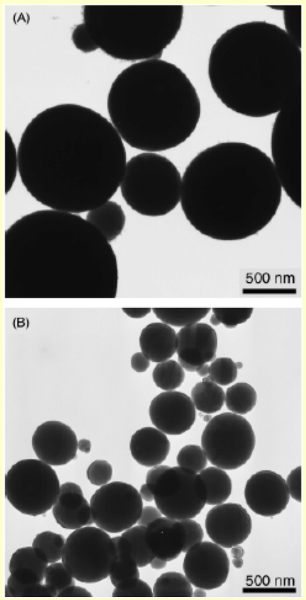

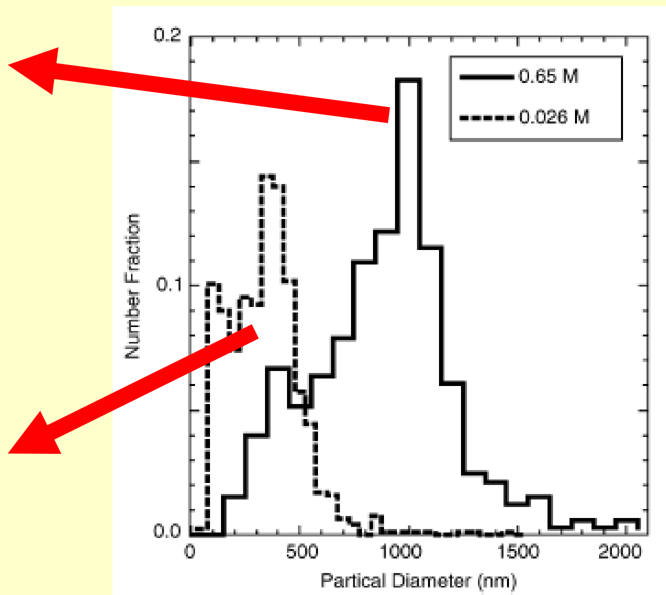

Flame Aerosol Process

Calcium phosphate nanoparticles Ca/P molar ratios 1.43 to 1.67

Synthesized by simultaneous combustion of
$Ca(OAc)_2$ + $OP(O^nBu)_3$ in a flame spray reactor

Fluoro-apatite and zinc or magnesium doped calcium phosphates
adding trifluoroacetic acid or metal carboxylates into the fuel

Nanoparticle morphology

At a molar ratio of Ca/P < 1.5 promoted the formation of dicalcium pyrophosphate ($Ca_2P_2O_7$)

Phase pure tricalcium phosphate TCP - $Ca_3(PO_4)_2$
obtained with a precursor Ca/P ratio of 1.52 after subsequent calcination at 900 °C

Micropores and the facile substitution of both anions and cations
Possible application as a biomaterial

Spray Pyrolysis

Tubular furnace reactor

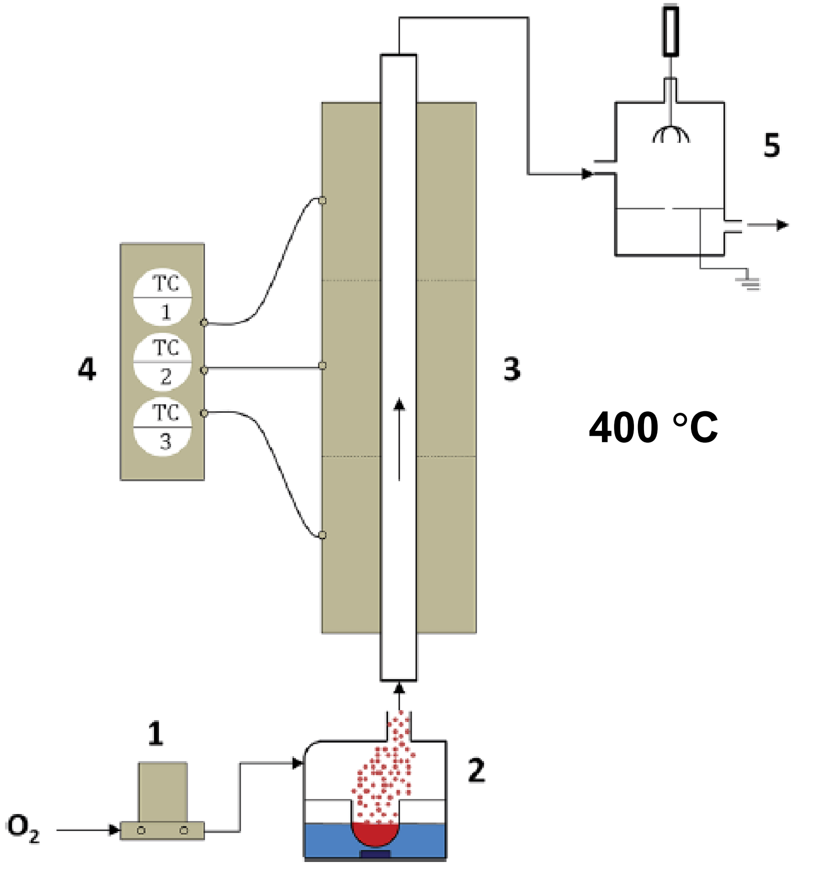

(1) mass flow controller – O_2 1 L/min
(2) ultrasonic nebulizer – aqueous solution 2 $Co(OAc)_2$: 1 $Ni(OAc)_2$
(3) 3-zone heater - 400 °C
(4) temperature controller
(5) electrostatic precipitator

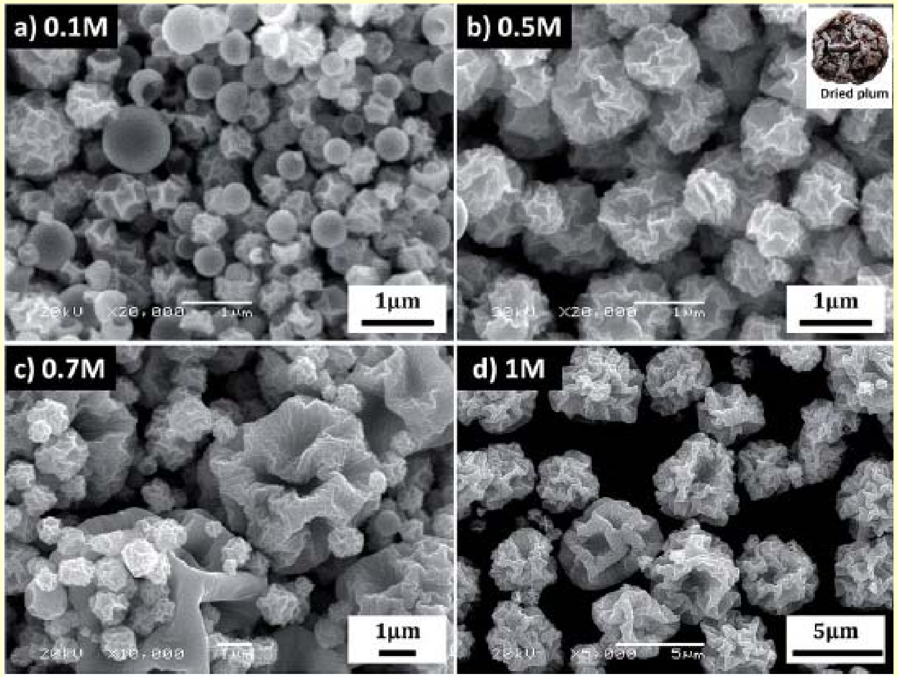

SEM micrographs of $NiCo_2O_4$ particles obtained from different concentrations of $Co(OAc)_2$ and $Ni(OAc)_2$ precursor solutions –
Lower concentration reduces particle size

Morphology Control

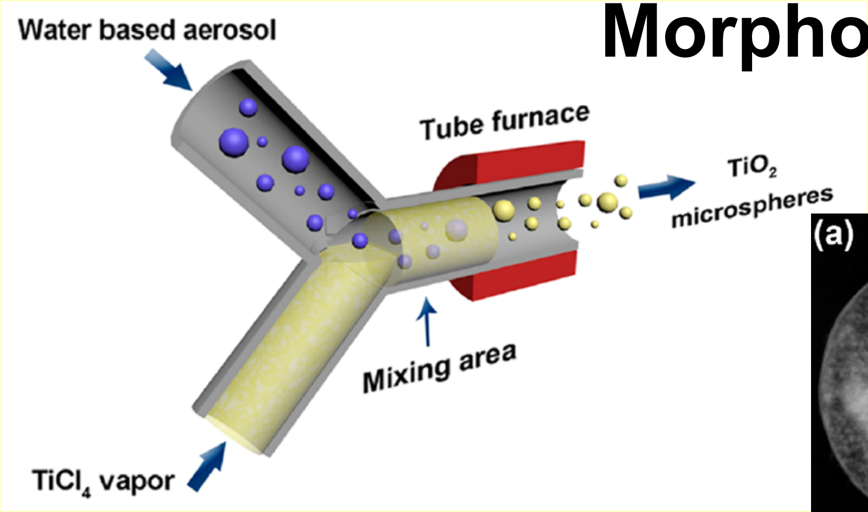

Rutile@Anatase core@shell microspheres

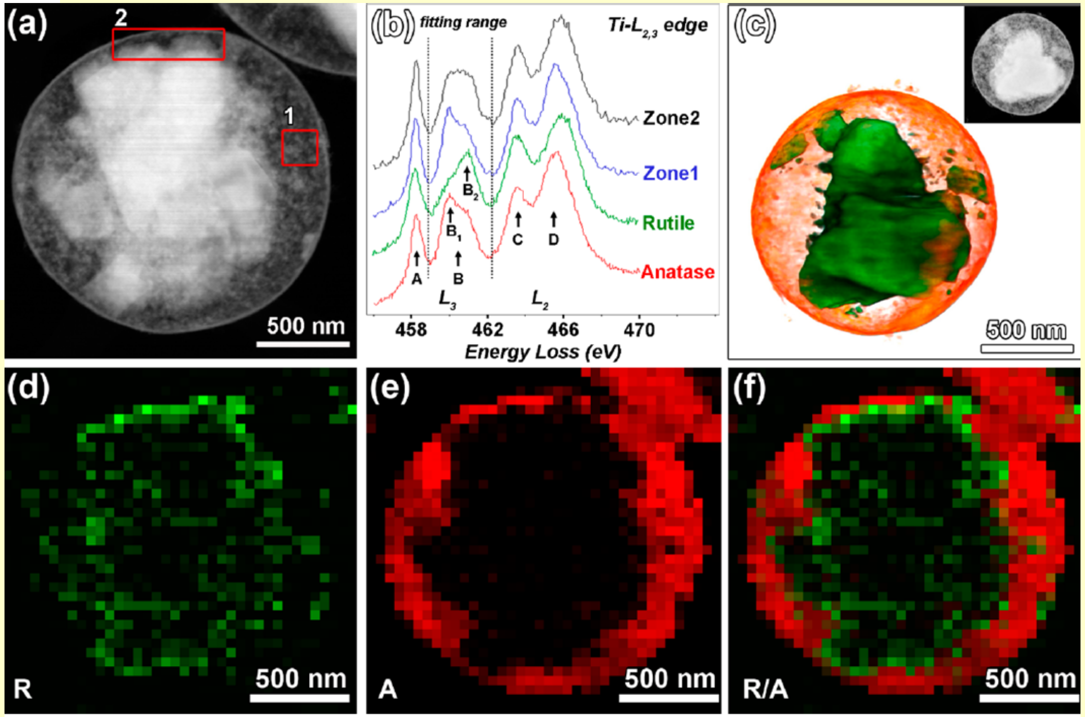

(a) HAADF-STEM of a rutile@anatase core@shell microsphere; (b) titanium L2,3 core-loss EELS spectra acquired from the indicated areas compared to reference TiO_2 polymorphs [rutile (green) and anatase (red)]

(d−f) EELS maps: (d) rutile (green), (e) anatase (red), and (f) rutile and anatase overlaid color map. (c) 3D tomographic reconstruction of another typical rutile@anatase core−shell microsphere, together with the corresponding HAADF-STEM image (inset)

Gas Phase Reactions

High-power CO_2 lasers

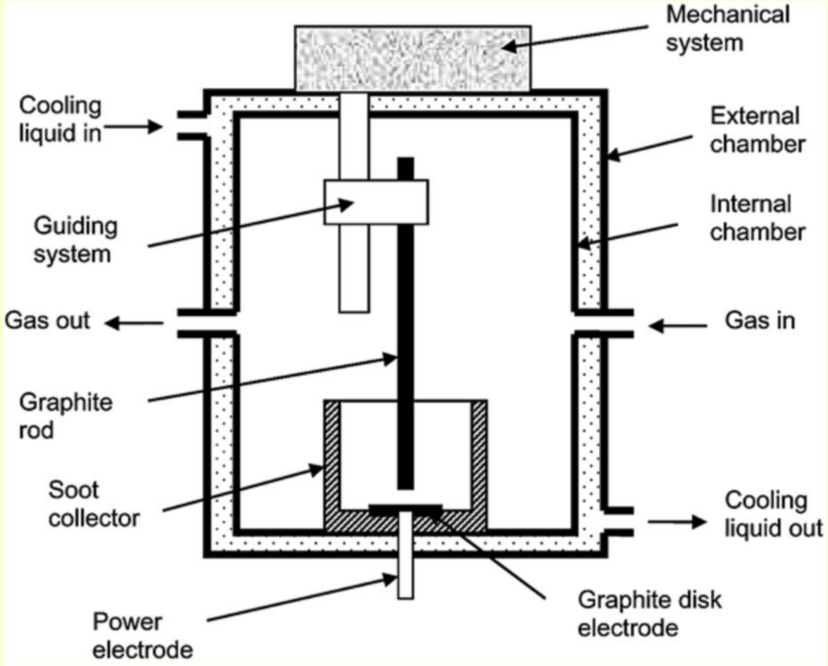

$3\ SiH_4 + 4\ NH_3 \rightarrow Si_3N_4 + 12\ H_2$

$HN(SiMe_3)_2 + NH_3 \rightarrow Si_3N_4 + SiC$

DC-Ar Plasma

$TiCl_4 + NH_3 \rightarrow TiN + HCl$

Electric arc synthesis (Krätschmer)

Graphite $\rightarrow C + C_2 + \ldots \rightarrow$ soot + $C_{60} + C_{70}$

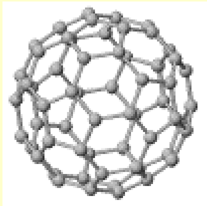

He atmosphere (100 torr),
U = 10–20 V, I = 0–250 A
Fullerene C_{60} extracted from the soot with toluene
Yields 1 – 10 %

Vapor Phase Transport Syntheses

Sealed glass tube reactors
Solid reactant(s) A + gaseous transporting agent B (O_2, Cl_2, I_2, CO…..)
Temperature gradient furnace ΔT ~ 50 - 1000 °C

A + B react at T_2 to form gaseous AB (g)
Equilibrium established $A (s) + B (g) \rightleftarrows AB (g)$
Equilibrium constant K
Gaseous transport of AB (g) to the other end
Concentration gradient of AB (g) = driving force for gaseous diffusion
AB (g) decomposes back to A (s) at T_1, crystals of pure A
Temperature dependent K
Equilibrium concentration of AB (g) changes with T, different at T_2 and T_1

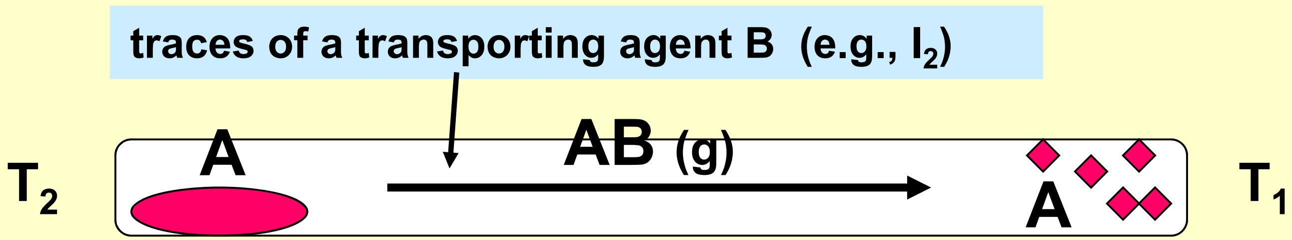

$A (s) + B (g) \longrightarrow AB (g)$ $A (s) + B (g) \longleftarrow AB (g)$

Vapor Phase Transport Syntheses

Whether T1 < T2 or T1 > T2 depends on the thermochemical balance of the reaction !
Transport can proceed from higher to lower or from lower to higher temperature

Example: Pt (s) + O_2 (g) $\rightleftarrows$ PtO_2 (g)

Endothermic reaction, PtO_2 forms at hot end, diffuses to cool end, deposits well formed Pt crystals, observed in furnaces containing Pt heating elements or thermocouples (thermometers)

Chemical vapor transport, $T_2 > T_1$, provides concentration gradient and thermodynamic driving force for gaseous diffusion of vapor phase transport agent AB (g)

Uses of VPT

- **Synthesis of new solid state materials**
- **Growth of single crystals**
- **Purification of solids**

Thermodynamics of VPT

van't Hoff equation

$$\ln K_2 - \ln K_1 = \ln \frac{K_2}{K_1} = \frac{\Delta H^0}{R}\left(\frac{1}{T_1} - \frac{1}{T_2}\right)$$

A (s) + B (g) ⇄ AB (g)

Reversible equilibrium needed: $\Delta G° = -RT\ \ln K_{eq} = \Delta H° - T\ \Delta S°$

*** Exothermic $\Delta H° < 0$**
Smaller T implies larger K_{eq}
AB (g) forms at cooler end, decomposes at hotter end of reactor

$W + 3\ Cl_2 \rightleftarrows WCl_6$ 400/1400 °C (exo)

$Ni + 4\ CO \rightleftarrows Ni(CO)_4$ 50/190 °C (exo)

*** Endothermic $\Delta H° > 0$**
Larger T implies larger K_{eq}
AB (g) forms at hotter end, decomposes at cooler end of reactor

$2\ Al + AlCl_3 \rightleftarrows 3\ AlCl$ 1000/600 °C (endo)

$4\ Al + Al_2S_3 \rightleftarrows 3\ Al_2S$ 1000/900 °C (endo)

Vapor Phase Transport Syntheses

Estimation of the thermochemical balance (ΔH) of a transport reaction:

$$ZnS_{(s)} + I_{2(gas)} \rightleftarrows ZnI_{2(gas)} + S_{(g)} \quad \Delta H = ??$$

$$Zn_{(s)} + I_{2(g)} \rightleftarrows ZnI_{2(gas)} \qquad \Delta H_f = -88 \text{ kJ mol}^{-1}$$

$$ZnS_{(s)} \rightleftarrows Zn_{(s)} + S_{(g)} \qquad -(\Delta H_f) = +201 \text{ kJ mol}^{-1}$$

$$\sum \quad ZnS_{(s)} + I_{2(gas)} \rightleftarrows ZnI_{2(gas)} + S_{(g)} \quad \Delta H = +113 \text{ kJ mol}^{-1}$$

Endothermic reaction, transport from hot to cold end!

Applications of VPT Methods

Purification/crystallization of metals: Van Arkel Method

$Cr\ (s) + I_2\ (g) \rightleftarrows CrI_2\ (g)$ Exothermic

Exothermic, CrI_2 (g) forms at cold end, pure Cr (s) deposited at hot end
Useful for Ti, Hf, V, Nb, Cu, Ta, Fe, Th
Removes metals from carbide, nitride, oxide impurities

$Ti + 2\ I_2 \rightleftarrows TiI_4$

$\Delta H = -376\ kJ\ mol^{-1}$

Exothermic:

transport from cold to hot

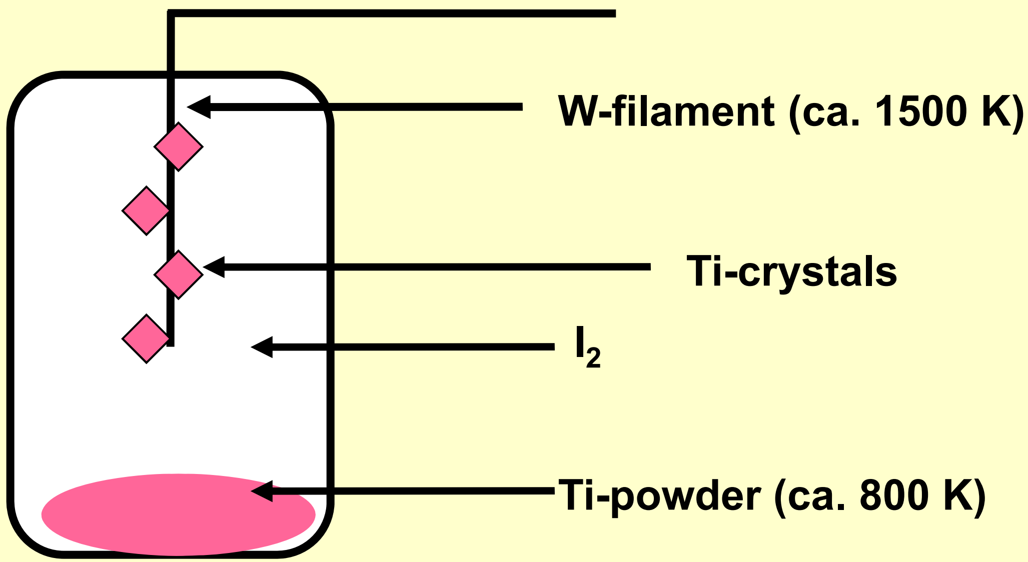

Applications of VPT Methods

Double Transport involving opposing Exothermic-Endothermic reactions

Endothermic:

$$WO_2\,(s) + I_2\,(g)\ (800\ ^\circ C) \rightleftarrows WO_2I_2\,(g)\ (1000\ ^\circ C)$$

Exothermic:

$$W\,(s) + 2\,H_2O\,(g) + 3\,I_2\,(g)\ (1000\ ^\circ C) \rightleftarrows WO_2I_2\,(g) + 4\,HI\,(g)\ (800\ ^\circ C)$$

The antithetical nature of these two reactions allows W/WO_2 mixtures to be separated at different ends of the gradient reactor using H_2O/I_2 as the transporting VP reagents

Applications of VPT Methods

Vapor Phase Transport for Synthesis

$A (s) + B (g) (T_1) \rightleftarrows (T_2) AB (g)$

$AB (g) + C (s) (T_2) \rightleftarrows (T_1) AC (s) + B (g)$

Concept: couple VPT with subsequent reaction to give overall reaction:

$A (s) + C (s) (T_2) \rightleftarrows (T_1) AC (s)$

Direct reaction sluggish even at high T

$SnO_2 (s) + 2\ CaO (s) \longrightarrow Ca_2SnO_4 (s)$ **Phosphor material for light-emitting diodes**

The reaction speeded up with CO as VPT agent:

$SnO_2 (s) + CO (g) \rightleftarrows SnO (g) + CO_2 (g)$

$SnO (g) + CO_2 (g) + 2\ CaO (s) \rightleftarrows Ca_2SnO_4 (s) + CO (g)$

Applications of VPT Methods

Direct reaction is sluggish:

Cr_2O_3 (s) + NiO (s) $\rightarrow$ $NiCr_2O_4$ (s) Magnetic materials

Cr_2O_3 (s) + 3/2 O_2 $\rightleftarrows$ 2 CrO_3 (g) Greatly enhanced rate with O_2

2 CrO_3 (g) + NiO (s) $\rightleftarrows$ $NiCr_2O_4$ (s) + 3/2 O_2 (g)

Overcoming Passivation Through VPT

2 Al (s) + 3 S (s) $\rightarrow$ Al_2S_3 (s) Passivating skin stops reaction

In presence of surface cleansing VPT agent I_2:

Endothermic:

Al_2S_3 (s) + 3 I_2 (g) (700 °C) $\rightleftarrows$ 2 AlI_3 (g) + 3/2 S_2 (g) (800 °C)

Applications of VPT Methods

Vapor Phase Transport for Synthesis

Zn (s) + S (s) $\rightarrow$ ZnS (s)   passivation prevents reaction to completion

Endothermic:

ZnS (s) + I_2 (g) (800 °C) $\rightleftarrows$ ZnI_2 (g) + ½ S_2 (g) (900 °C)

VPT Synthesis of $ZnWO_4$ from WO_3 and ZnO
a phosphor host crystal for Ag^+, Cu^+, Mn^{2+}

WO_3 (s) + 2 Cl_2 (g) (980 °C) $\rightleftarrows$ WO_2Cl_2 (g) + Cl_2O (g) (1060 °C)

ZnO (s) + WO_2Cl_2 (g) + Cl_2O (g) (1060 °C) $\rightleftarrows$ $ZnWO_4$ (s) + Cl_2 (g)

Growth of epitaxial GaAs films or single crystals by VPT

GaAs (s) + HCl (g) $\rightleftarrows$ GaCl (g) + ½ H_2 (g) + ¼ As_4 (g)   Endothermic

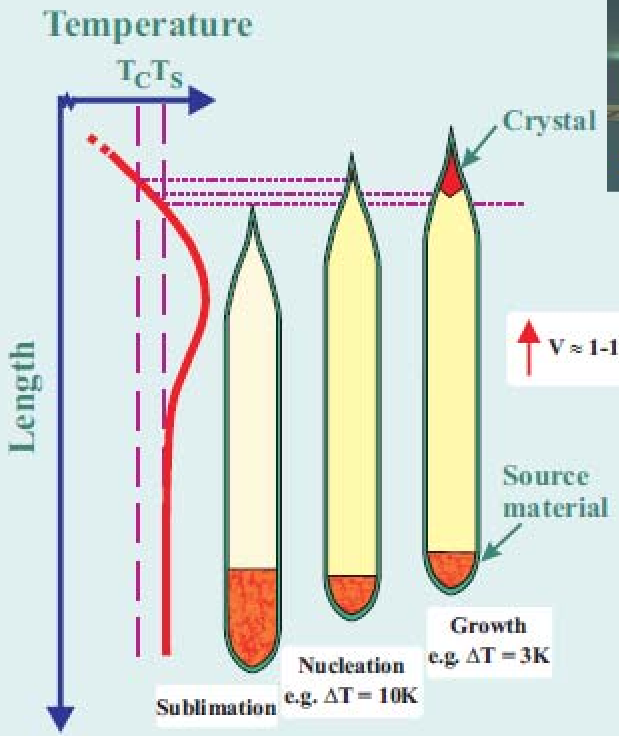

T_S = source temperature
T_C = crystal temperature
$\Delta T = T_S - T_C$

ZnSe, ZnTe, CdS

1. Purification by sublimation
2. Synthesis
3. Sublimation or chemical vapor transport

Crystals grown:

ZnO, ZnSe, ZnTe, CdS, CdSe, Ag_2S, CuCl, CuBr, CuI, AgI, TiO_2, C_{60}, C_{70}, Zn, Cd, Mg etc.

KBr GeS TlBr

A view of vapor growth equipment

Laser-induced Homogeneous Pyrolysis

Laser wavelength
10.60 ± 0.05 μm

$$Fe(CO)_5 \rightarrow Fe + 5\,CO$$

- **Overlap between the vertical reactant gas stream and the horizontal laser beam**
- **Reaction zone away from the chamber walls**
- **Nucleation of nanoparticles**
- **Less contamination**
- **Narrow size distribution**

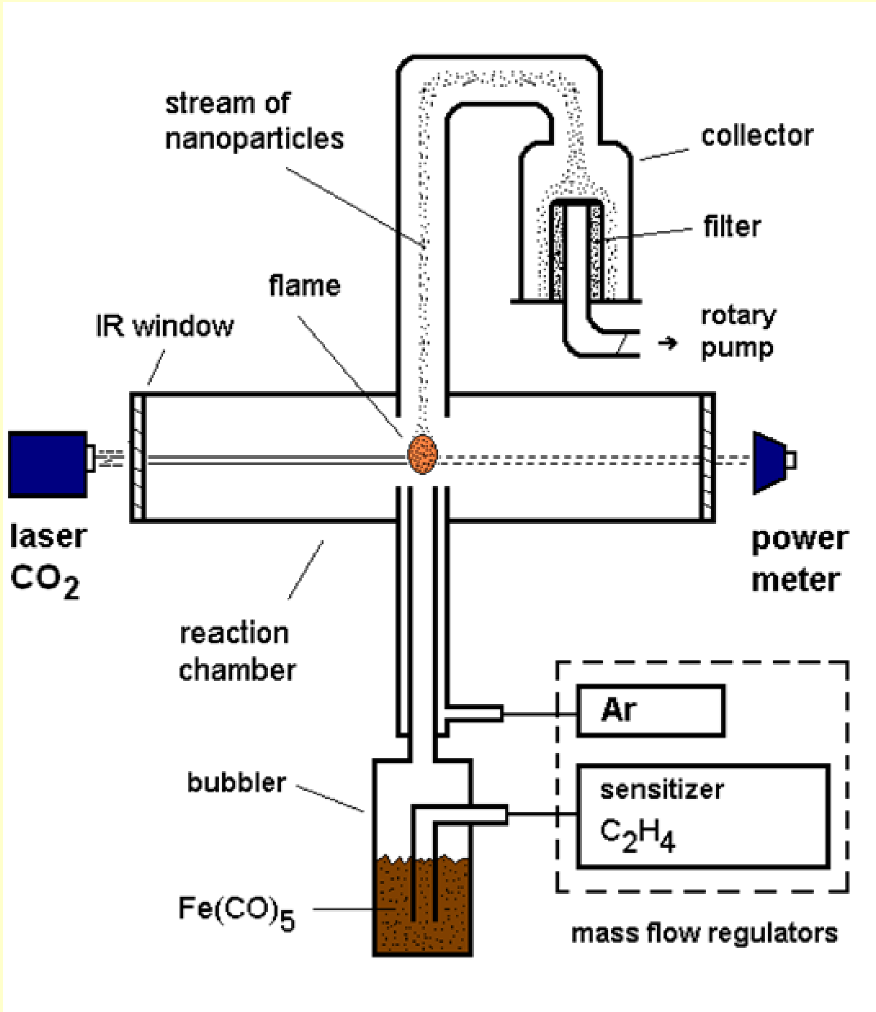

$$C_2H_4 + h\nu \rightarrow C_2H_4^*$$

Excitation energy transferred to vibrational-translational modes

⇒ T increases

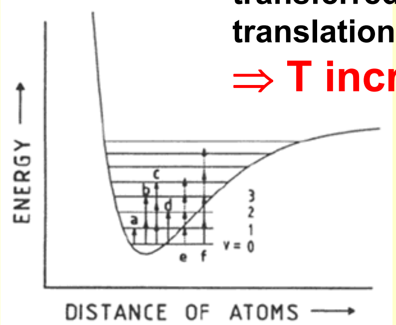

Sensitizer

SF_6
948 cm^{-1}

Isopropanol
958 cm^{-1}

Iron-oxide Nanoparticles by Laser-induced Homogeneous Pyrolysis

$$2\,Fe(CO)_5 + 3\,N_2O \rightarrow Fe_2O_3 + 10\,CO + 3\,N_2$$

TEM

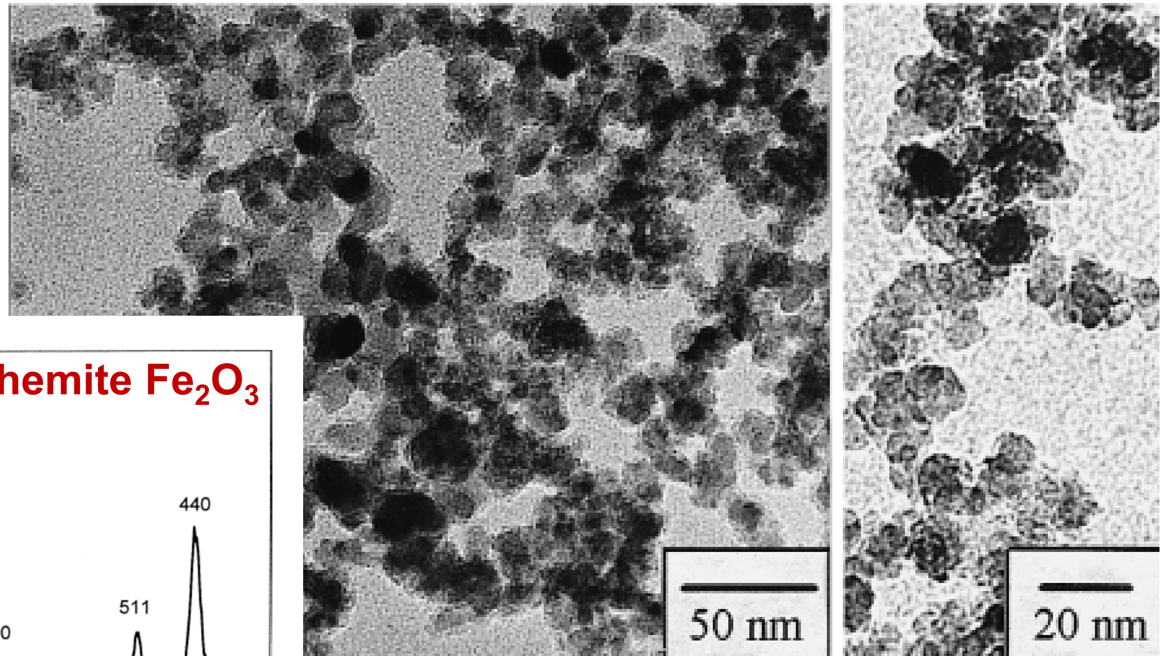

TEM micrographs of the synthesised γ-Fe_2O_3 particles.